CAMBRIDGE
Cambridge University Press & Assessment
978-1-108-49076-4 — Multi-scale (Time and Mass) Dynamics of Space Objects (IAU S364)
Edited by Alessandra Celletti, Cristian Beaugé, Cătălin Galeş, Anne Lemaître
Excerpt
More Information

Multi-scale (time and mass) dynamics of space objects
Proceedings IAU Symposium No. 364, 2022
A. Celletti, C. Galeş, C. Beaugé, A. Lemaitre, eds.
doi:10.1017/S174392132100140X

Dynamical constraints on the evolution of the inner asteroid belt and the sources of meteorites

Stanley F. Dermott[1], Dan Li[2] and Apostolos A. Christou[3]

[1]Department of Astronomy, University of Florida, Gainesville, FL 32611, US
email: sdermott@ufl.edu

[2]NSF's National Optical-Infrared Astronomy Research Laboratory, Tucson, AZ 85719, US
email: dan.li@noirlab.edu

[3]Armagh Observatory and Planetarium, College Hill, Armagh, BT61 9DG
email: Apostolos.Christou@armagh.ac.uk

Abstract. We have shown that in the inner belt the loss of asteroids from the ν_6 secular resonance and the 3:1 Jovian mean motion resonance accounts for the observation that the mean size of the asteroids increases with increasing orbital inclination. We have used that observation to constrain the Yarkovsky loss timescale and to show that the family asteroids are embedded in a background population of old ghost families. We argue that all the asteroids in the inner belt originated from a small number of asteroids and that the initial mass of the belt was similar to that of the present belt. We also show that the observed size frequency distribution of the Vesta asteroid family was determined by the action of Yarkovsky forces, and that the age of this family is comparable to the age of the solar system.

Keywords. asteroids

1. Introduction

Small fragments of many asteroids exist in our meteorite collections and while these fragments provide invaluable information on the origin and evolution of the remnants of the primitive building blocks that formed the rocky planets, some important dynamical questions remain unanswered. Ideally, we would like to link specific meteorites or meteorite classes to known asteroids. In one case at least, given the strong links between 4 Vesta and the HED meteorites, that goal has been achieved (McSween *et al.* 2013). We also have small samples of material from the near-Earth asteroid (NEA) Itokawa and soon we expect to have samples from the NEAs Ryugu and Bennu. However, these small NEAs are rubble-pile asteroids that originate from the collisional disruption of much larger main-belt asteroids. One aim of this paper is to discuss some of the dynamical constraints on the likely number of precursor asteroids in the inner main belt (IMB) that are the root sources of a large fraction of the NEAs and meteorites.

We assume that the asteroids accreted in two separate reservoirs of carbonaceous (CC) and non-carbonaceous (NC) material, interior and exterior to their current locations, and were then scattered by planetary perturbations into the present belt (Walsh *et al.* 2011; Kruijer *et al.* 2017). We also assume that after all planetary migration and the scattering that resulted from that migration ceased, further evolution of the dynamically excited belt was driven by: (1) the collisional and (2) the rotational destruction of asteroids (Dohnanyi 1969; Jacobson *et al.* 2014); (3) chaotic orbital evolution (Wisdom 1985;

© The Author(s), 2022. Published by Cambridge University Press on behalf of International Astronomical Union. This is an Open Access article, distributed under the terms of the Creative Commons Attribution licence (https://creativecommons.org/licenses/by/4.0/), which permits unrestricted re-use, distribution, and reproduction in any medium, provided the original work is properly cited.

© in this web service Cambridge University Press & Assessment www.cambridge.org

CAMBRIDGE
Cambridge University Press & Assessment
978-1-108-49076-4 — Multi-scale (Time and Mass) Dynamics of Space Objects (IAU S364)
Edited by Alessandra Celletti, Cristian Beaugé, Cătălin Galeş, Anne Lemaître
Excerpt
More Information

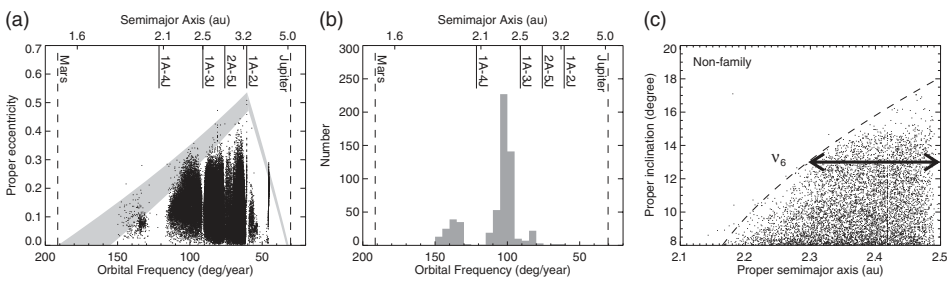

Figure 1. Panel (a): Scatter plot of the proper eccentricity e and the semimajor axis, a of the asteroids in the IMB with absolute magnitude $H < 15$. The shaded zone on the left is the Mars-crossing zone. Asteroids in that zone can, over time, cross the orbit of Mars. Panel (b): Histogram of the semimajor axes of the asteroids in the Mars-crossing zone. Panel (c): non-family asteroids in the IMB with $H < 16.5$ and high proper inclinations (Dermott *et al.* 2021).

Farinella *et al.* 1994; Morbidelli & Nesvorný 1999; Minton & Malhotra 2010); and (4) Yarkovsky-driven transport of small asteroids to the escape hatches located at orbital resonances (Migliorini *et al.* 1998; Farinella & Vokrouhlický 1999; Vokrouhlický & Farinella 2000). Insight into this dynamical evolution and estimates of the loss timescales are gained from an analysis of: (1) the observed variations with asteroid size of the mean orbital inclinations and eccentricities of the non-family asteroids; and (2) the size-frequency distributions of the small asteroids in the major families (Dermott *et al.* 2018; Dermott *et al.* 2021); (3) the cosmic-ray exposure ages of meteorites (Eugster *et al.* 2006); (4) the spin directions of near-Earth asteroids (Greenberg *et al.* 2020); and (5) the distribution of family asteroids in $a - 1/D$ space, where D is the asteroid diameter.

2. Asteroid size - orbital element correlations

The orbital eccentricities of main-belt asteroids are largely capped by the Mars-crossing zone (Fig. 1a) indicating that Mars has scattered some asteroids into the inner solar system. Most of the asteroids in the crossing-zone are in the inner main belt (IMB) (Fig. 1b), suggesting that the IMB is a major source of near-Earth asteroids (NEAs) and meteorites, a conclusion that is supported by the results of numerical investigations of the likely escape routes (Gladman *et al.* 1997; Granvik *et al.* 2017, 2018). Using the Hierarchical Clustering Method (HCM) developed by Zappala *et al.* (1990), Nesvorný (2015) has classified about half of the asteroids in the IMB with absolute magnitudes, $H < 16.5$ as family asteroids. But this fraction is an underestimate because some of the remaining asteroids are halo asteroids (Nesvorný *et al.* 2015), that is, they are also family asteroids, but because of the unavoidable limitations of the HCM it is not possible to classify these asteroids unambiguously. The remaining asteroids that are neither family nor halo asteroids are currently classified as non-family and an understanding of the evolution of the asteroid belt is not complete without an understanding of the nature and origin of these unclassified asteroids.

The family and halo asteroids are, by definition, tightly clustered in proper orbital element space. However, the family asteroids in that space are embedded in a background population of asteroids that could be members of old ghost families with dispersed orbital elements. To explore this background population, we need to find windows in orbital element space that are not obscured by the asteroids in the major families. Fortunately, one very large window exists in the IMB where all the asteroids in the major families and their halos have proper orbital inclinations, $I < 9$ *deg* (Dermott *et al.* 2018). In Fig. 1c, we see that the remaining non-family asteroids in the IMB with $I > 9$ *deg* are bound in $a - I$ space by the ν_6 secular resonance and the 3:1 Jovian mean motion resonance. These

© in this web service Cambridge University Press & Assessment www.cambridge.org

CAMBRIDGE
Cambridge University Press & Assessment
978-1-108-49076-4 — Multi-scale (Time and Mass) Dynamics of Space Objects (IAU S364)
Edited by Alessandra Celletti, Cristian Beaugé, Cătălin Galeş, Anne Lemaître
Excerpt
More Information

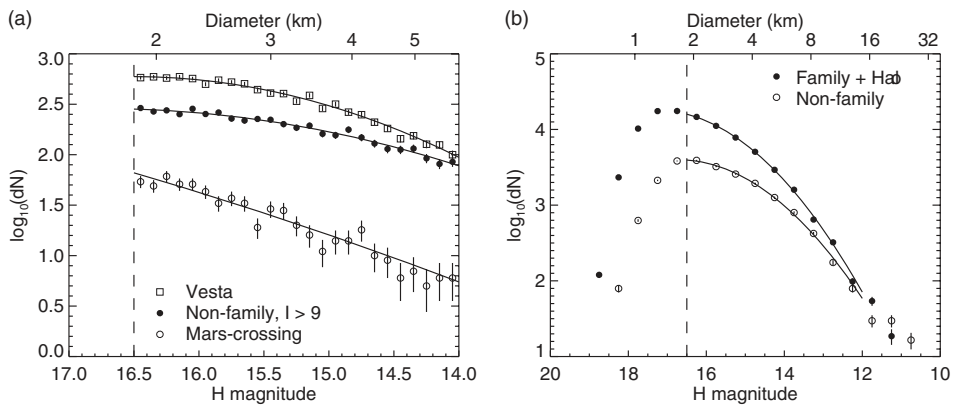

Figure 2. Panel (a): Quadratic polynomial fits to the SFDs of the asteroids in the Vesta family, for non-family asteroids with high inclinations ($I > 9\ deg$), and for asteroids in the Mars-crossing zone. Panel (b): Comparison of the SFD of the non-family asteroids in the IMB with an estimate of the SFD of the family asteroids when combined with the asteroids in their halos.

resonances are two of the major escape hatches for asteroids in the IMB (Gladman *et al.* 1997; Granvik *et al.* 2017, 2018), but a third escape route is provided by a dense web of high-order Martian and Jovian resonances (Morbidelli & Nesvorný 1999; Milani *et al.* 2014) and we have argued that there is observational evidence that these high-order resonances also provide a significant loss mechanism (Dermott *et al.* 2021).

The size-frequency distribution (SFD) of the high inclination non-family asteroids shown in Fig. 2a shows a lack of small asteroids that is consistent with these asteroids being members of old ghost families that have lost small asteroids through collisional and rotational disruptions and the action of Yarkovsky forces. By assuming that the number density in $a - I$ space of the high-inclination, non-family asteroids shown in Fig. 1c applies to the IMB as a whole, we have shown that the fraction of asteroids in the IMB with $H < 16.5$ that are members of the major families or their halos is 76% and that the remaining 24% of the asteroids in the IMB are members of old ghost families (Dermott *et al.* 2021). If we further assume that the SFD of the high-inclination, non-family asteroids shown in Fig. 2a applies to all the non-family asteroids in the IMB and that the SFD of the halo asteroids (as a whole) is the same as that of the family members, then we can compare the SFD of the ghost family members with that of the family members and their halos. Accepting these simplifying assumptions, Fig. 2b shows that the smaller asteroids in the IMB with $H \sim 16$ are predominantly members of the major families. However, for asteroids with $H \lesssim 12$ and diameters, $D \gtrsim 16\ km$ this is not the case. This has several implications. Firstly, the probability of an asteroid that is currently classified as a family member being a family interloper increases with increasing asteroid size. Secondly, the fractions of the asteroids that are currently classified as S-type or C-type, etc., could change with asteroid size (see DeMeo & Carry 2014). Thirdly, our estimate of the number of asteroids that are the root sources of the NEAs and meteorites that originate from the IMB depends on the typical size of the asteroids whose disruption resulted in the injection of NEAs and meteorites into the inner solar system. Here, because the cosmic ray exposure ages of meteorites (Eugster *et al.* 2006) are much less than the ages of the asteroid families, we assume that the NEAs and meteorites do not originate directly from the initial disruptions of the root precursor asteroids, that is, from the events that formed the families, but from secondary disruptions of the family members. If the secondary asteroids were totally disrupted and typically had diameters

© in this web service Cambridge University Press & Assessment www.cambridge.org

CAMBRIDGE
Cambridge University Press & Assessment
978-1-108-49076-4 — Multi-scale (Time and Mass) Dynamics of Space Objects (IAU S364)
Edited by Alessandra Celletti, Cristian Beaugé, Cătălin Galeş, Anne Lemaître
Excerpt
More Information

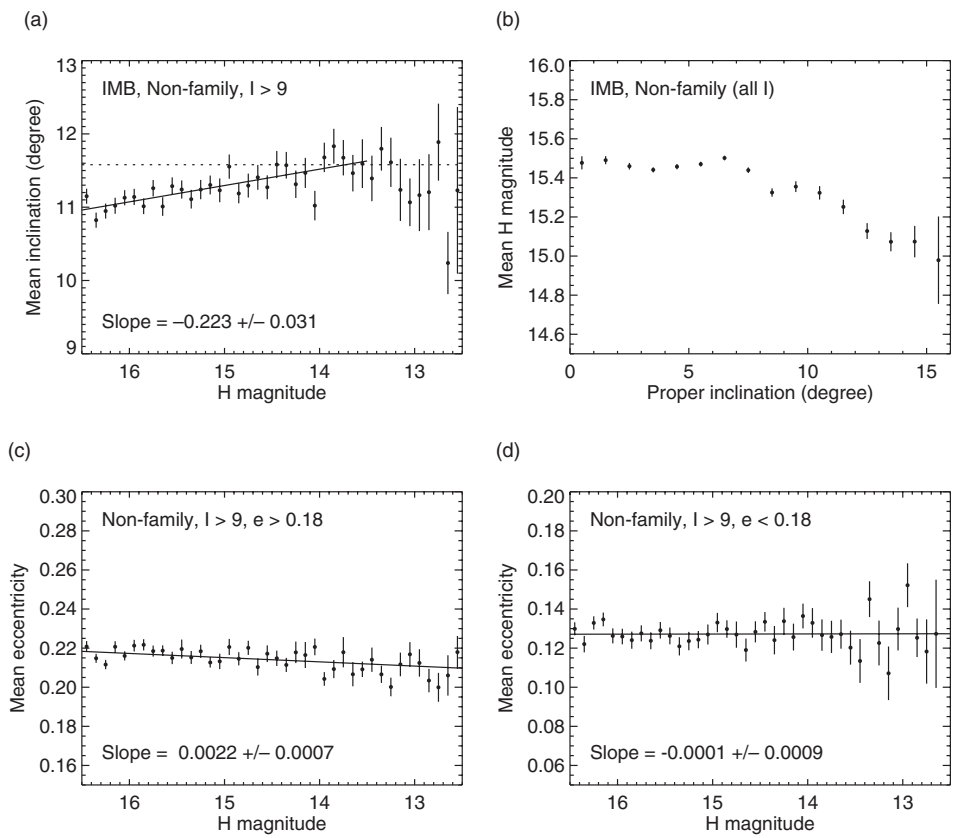

Figure 3. Panel (a): Variation with absolute magnitude, H of the mean proper inclination of the high inclination ($I > 9$ *deg*), non-family asteroids. The data is shown binned in H, but the slope has been determined from the individual points in the range $16.5 > H > 13.5$. Panel (b): Variation with proper inclination, I of the mean absolute magnitude, H of the all the non-family asteroids in the IMB. Panel (c): Variation with absolute magnitude, H of the mean proper eccentricity of the high inclination ($I > 9$ *deg*), non-family asteroids with $e > 0.18$. Panel (d) A similar plot to Panel (c) for those asteroids with $e < 0.18$ (Dermott *et al.* 2021).

$\sim 1\ km$, as suggested by Jenniskens (2020), then these asteroids were most likely members of the 5 or 6 major families currently dominating the IMB in that size range (Fig. 2b). This estimate of the number of precursors is small and could be reduced even further by considering the proximity of the major families to the most likely escape hatches. However, if the meteorite sources were larger, then we must also consider the asteroids in the ghost families as possible precursors, and this increases our estimated number of root precursors to $\lesssim 20$ (Dermott *et al.* 2021).

Asteroids are lost from the IMB through at least four mechanisms: collisional and rotational destruction, chaotic orbital evolution, and Yarkovsky-driven transport of small asteroids to the resonant escape hatches. The timescales of these loss mechanisms are uncertain and there is a need for observational constraints. Of particular interest are the observed correlations between the mean asteroid sizes and their proper orbital elements. In Fig. 3a, we see that the mean proper inclination of the high-inclination ($I > 9$ *deg*), non-family asteroids in the IMB increases with increasing asteroid size. In contrast, in

© in this web service Cambridge University Press & Assessment www.cambridge.org

CAMBRIDGE
Cambridge University Press & Assessment
978-1-108-49076-4 — Multi-scale (Time and Mass) Dynamics of Space Objects (IAU S364)
Edited by Alessandra Celletti, Cristian Beaugé, Cătălin Galeş, Anne Lemaître
Excerpt
More Information

Fig. 3c we see that the mean proper eccentricity of the high-eccentricity asteroids (that also have high inclination), increases with decreasing asteroid size. The size-inclination correlation can be accounted for by the action of Yarkovsky forces driving small asteroids to the two bounding resonances (Dermott *et al.* 2021). The length of the escape route (Fig. 1c) decreases with increasing inclination and this leads, inevitably, to a correlation between the sizes and inclinations of the remaining asteroids. The distribution of the asteroids in $a - I$ space shown in Fig. 1c appears to be approximately uniform. If we assume that the initial distribution was also uniform, that is, not dependent on a or I, then the observed size-inclination correlation is determined by the Yarkovsky timescale alone and this timescale can be determined without knowing the initial SFD. We write

$$\frac{1}{a}\frac{da}{dt} = \pm\left(\frac{1}{T_{\rm Y}}\right)\left(\frac{1\,km}{D}\right)^{\alpha}, \tag{1}$$

where $T_{\rm Y}$ is the Yarkovsky timescale and the coefficient α is determined by the size dependence of the Yarkovsky force. The other loss mechanisms that do not depend on the orbital inclination include the net effect of catastrophic destruction and creation, and rotational disruption. These loss mechanisms are size dependent and should be modeled separately, but we are able to show that, in the size range that we model, Yarkovsky loss is the dominant loss mechanism and therefore it is expedient to reduce the number of variables in our models by writing

$$\frac{1}{N(D)}\frac{dN(D)}{dt} = -\left(\frac{1}{T_{\rm L}}\right)\left(\frac{1\,km}{D}\right)^{\beta}, \tag{2}$$

where $T_{\rm L}$ is the timescale of the combined inclination-independent loss mechanisms and $N(D)$ is the number of asteroids of diameter D.

Some of our model results, obtained using both loss mechanisms, are shown in Fig. 4. By adjusting the values of the five parameters b, α, $T_{\rm Y}$, β, $T_{\rm L}$, we can account for both the observed size-inclination correlation (Figs. 4c and 4f) and the observed SFD (Fig. 4b). These results show that for asteroids with absolute magnitudes in the range $13.5 < H < 16.5$, Yarkovsky transport of asteroids to the resonant escape hatches is the dominant loss mechanism (Fig. 4a). This conclusion is supported by the model results shown in Figs. 4d and 4e in which we use the Yarkovsky loss mechanism alone. For asteroids with $H < 16.5$ the inclination-independent asteroid loss mechanism has only a small effect on the fit for the SFD, and no effect on the observed asteroid size-inclination correlation. There is a large difference to the SFD fit for those asteroids with $H > 16.5$, but, at present, these very small asteroids are observationally incomplete. When the IMB completeness level has been extended from $H = 16.5$ to, say, $H = 18$, we will be able to constrain the loss timescales for the collisional and rotational disruption of the asteroids.

Using both loss mechanisms, we calculate that if these mechanisms have operated without change over the age of the solar system, then the Yarkovsky loss timescale, $T_{\rm Y}$ needed to account for the size-inclination correlation is 13.4 Gyr. This timescale is unacceptably longer than the result, $T_{\rm Y} \approx 4$ Gyr for asteroids with $a = 2.4$ au derived from the value that Greenberg *et al.* (2020) obtained from an analysis of the orbital evolution of 247 small NEAs. If the Yarkovsky timescale was as short as 4 Gyr, then many more asteroids would have been lost from the IMB and the size-inclination correlation would have been much stronger. We have argued that the most likely explanation for this large discrepancy is that the asteroids in the IMB are not as old the solar system but are collision products and members of old ghost families. However, this explanation for the observed size-inclination correlation needs to be explored further. Previously, we

© in this web service Cambridge University Press & Assessment www.cambridge.org

CAMBRIDGE
Cambridge University Press & Assessment
978-1-108-49076-4 — Multi-scale (Time and Mass) Dynamics of Space Objects (IAU S364)
Edited by Alessandra Celletti, Cristian Beaugé, Cătălin Galeş, Anne Lemaître
Excerpt
More Information

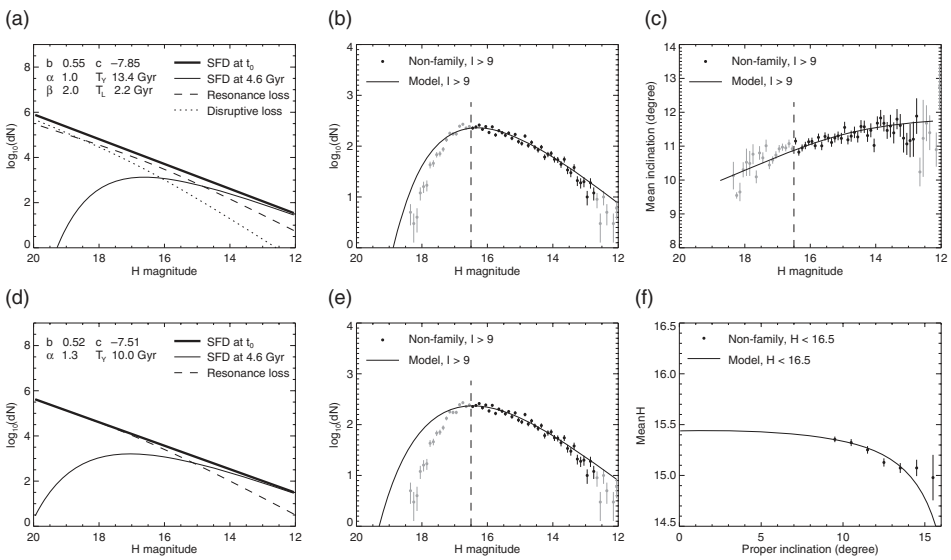

Figure 4. Models for the depletion of all the high-inclination, non-family asteroids in the IMB due to a Yarkovsky force that changes the semimajor axes on a timescale $T_{\rm Y}$, and all other loss mechanisms that do not depend on the proper inclination, I and result in the loss of asteroids on a timescale $T_{\rm L}$. α and β describe the dependence of these two timescales on the asteroid diameter.

argued that the asteroid size-orbital element correlations of the non-family asteroids in the IMB are evidence for the existence of ghost families (Dermott *et al.* 2018), because if we had, say, two families and the members in one family had a common inclination that was different from the common inclination of the members in the second family, and if these two families had different SFDs, then merging these two families could result in a ghost family with correlated inclinations and sizes. The difference between these two ideas is that the Yarkovsky loss model results, inevitably, in a size-inclination correlation of predictable sign and magnitude, whereas with the second idea a correlation of unpredictable sign and magnitude is only a possibility. If the number of merged families increases, then the possibility of a significant correlation due to the second mechanism alone decreases. However, what these two ideas have in common is that they both argue for the existence of ghost families, and we now need to examine other evidence for the existence of these families.

Figure 5 is a scatter plot of the high-inclination, IMB asteroids in $e - I$ space. Using the WISE albedos (Masiero *et al.* 2014), these asteroids have been separated into CC and NC groups. About 12% of the asteroids are members of small families (Figs. 5a and 5b). The remaining 88% (Figs. 5c and 5d) are non-family asteroids. Inspection of this figure shows that some of the CC non-family asteroids could be halo asteroids originating from the Klio and Chaldaea families, but some other apparent clumps could be large ghost families. The SFDs of the non-family CC and NC asteroids are shown in Fig. 6. These SFDs are significantly different which could indicate families of different ages. However, this is not a reliable conclusion because only about half of the IMB asteroids with $H < 16.5$ have WISE albedos and therefore the data set is incomplete and not bias free. A more reliable indication of the existence of ghost families is the observation that the CC and NC asteroids have markedly different mean eccentricities and inclinations (Dermott *et al.* 2021).

© in this web service Cambridge University Press & Assessment www.cambridge.org

CAMBRIDGE
Cambridge University Press & Assessment
978-1-108-49076-4 — Multi-scale (Time and Mass) Dynamics of Space Objects (IAU S364)
Edited by Alessandra Celletti, Cristian Beaugé, Cătălin Galeş, Anne Lemaître
Excerpt
More Information

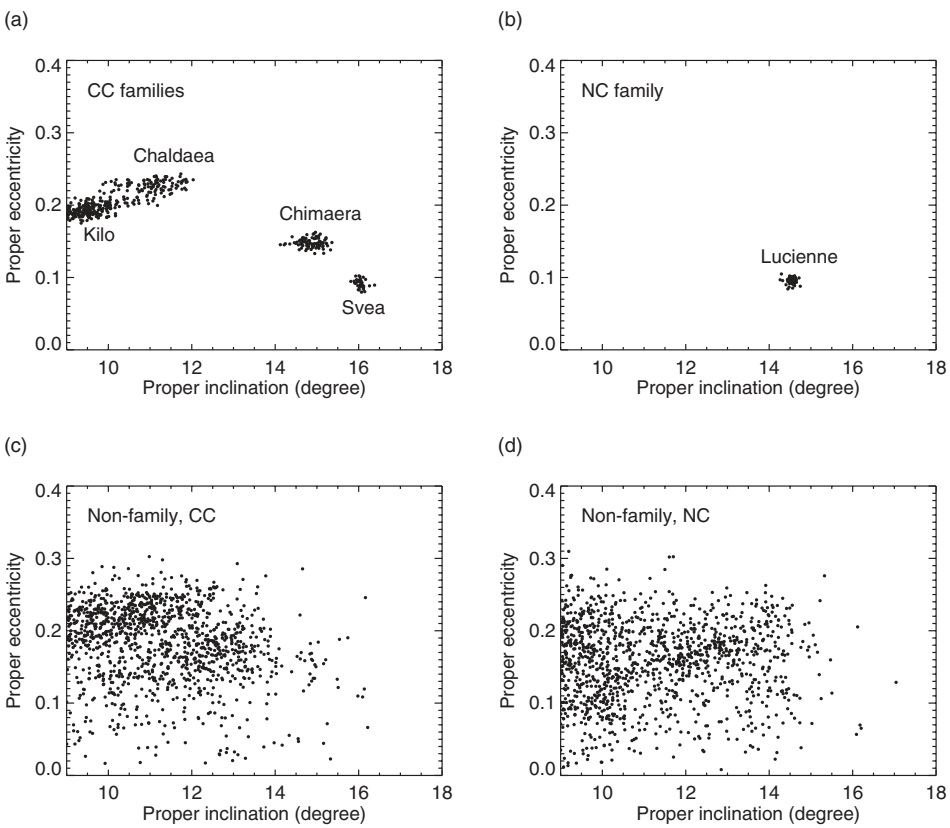

Figure 5. The asteroids in the IMB with high inclinations have been divided into two groups of CC and NC asteroids according to their WISE albedos, A (Masiero *et al.* 2014). CC have $A < 0.13$ and NC have $A > 0.13$. The panels show e and I scatter plots of all the asteroids with $H > 16.5$ divided into CC and NC family and non-family groups.

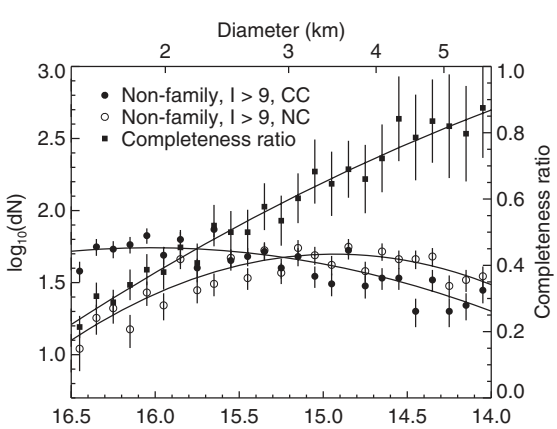

Figure 6. Comparison of the SFDs of the CC and NC non-family asteroids in the IMB with $I > 9$ *deg* and $H < 16.5$. The completeness ratio is the fraction of the asteroids with WISE albedos.

© in this web service Cambridge University Press & Assessment www.cambridge.org

CAMBRIDGE
Cambridge University Press & Assessment
978-1-108-49076-4 — Multi-scale (Time and Mass) Dynamics of Space Objects (IAU S364)
Edited by Alessandra Celletti, Cristian Beaugé, Cătălin Galeş, Anne Lemaître
Excerpt
More Information

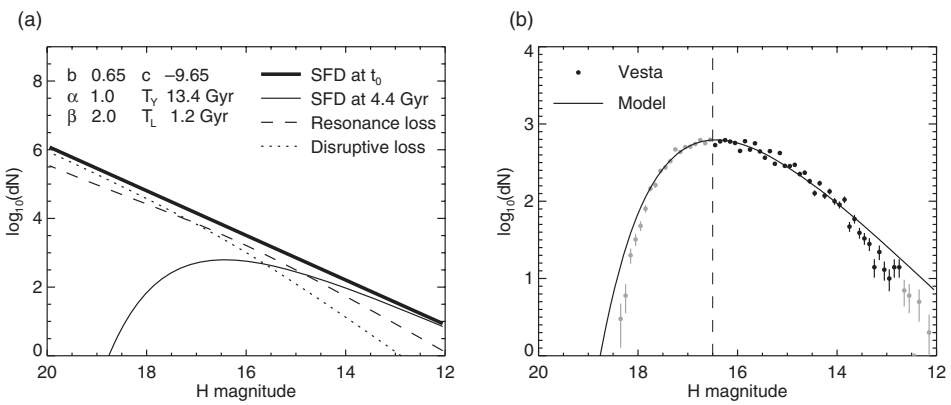

Figure 7. Panel (a): model for the loss of the Vesta family asteroids due to a Yarkovsky force that changes the semimajor axis on a timescale $T_{\rm Y}$, and to all other loss mechanisms that do not depend on the proper inclination that change the semimajor axis on a timescale $T_{\rm L}$. α and β describe the dependence of these timescales on the asteroid diameter, D. The constant b is the slope of the initial SFD and c is a normalizing constant that determines the total number of asteroids in the distribution.

3. The age of the Vesta asteroid family

The asteroid families were created either by collisional disruptions or by cratering events on large asteroids. In either case, if we assume that the SFD of the small asteroids in a family was initially linear on a log-log scale, as observed for the young Massalia family, then our models allow us to determine the age of the family and the initial slope, b of the incremental SFD that we assume had the form

$$\log dN = bH + c, \tag{3}$$

where dN is the number of asteroids in a box of width dH and c is a constant for asteroids with the same albedo. Because the asteroids in a family have, by definition, approximately the same inclination, and because the slope, b of the initial SFD is an unknown parameter, we only have one observational constraint on our model and that is the current SFD. Model results for the SFD of the Vesta family (Fig. 2) are particularly interesting. This family was probably formed by the impact that created the giant $\sim$500 km diameter and $\sim$20 km deep Rheasilvia basin that overlies and partially obscures the smaller ($\sim$400 km diameter) and older Veneneia crater (Marchi *et al.* 2012). Our model results are shown in Fig. 7. We allow that the age of the family, $t_{\rm Vesta}$, the initial slope of the SFD, b, and the timescale of the inclination-independent loss mechanism, $T_{\rm L}$, are free parameters, but set $\alpha = 1$, $\beta = 2$ and $T_{\rm Y}$ to the best-fitting value derived from the model for the high-inclination ($I > 9$ deg), non-family asteroids shown in Fig. 4. The results are only partly satisfactory because our best-fit solution has $b = 0.65$ which is slightly greater than the upper limit, $b = 0.6$, determined by the condition that the total mass in the distribution cannot be infinite (Durda & Dermott 1997). Noting that our models only derive ratios of timescales, our best model (Fig. 7) gives

$$t_{\rm Vesta}/T_{\rm Y} = 0.33 \pm 0.015. \tag{4}$$

If we assume that the mean density of the Vestoids is 2850 $kg\ m^{-3}$ (Jenniskens *et al.* 2021) - a value that is larger than the density of 2000 $kg\ m^{-3}$ assumed in our earlier paper (Dermott *et al.* 2021), then using the Greenberg *et al.* (2020) NEA observations and their estimate that the thermal efficiency, $\xi = 0.12$, we estimate that $T_{\rm Y} = 6$ Gyr and $t_{\rm Vesta} = 2.0 \pm 0.1$ Gyr. This age is greater than the age $\sim$1.3 Gyr obtained from Vesta

© in this web service Cambridge University Press & Assessment www.cambridge.org

CAMBRIDGE
Cambridge University Press & Assessment
978-1-108-49076-4 — Multi-scale (Time and Mass) Dynamics of Space Objects (IAU S364)
Edited by Alessandra Celletti, Cristian Beaugé, Cătălin Galeş, Anne Lemaître
Excerpt
More Information

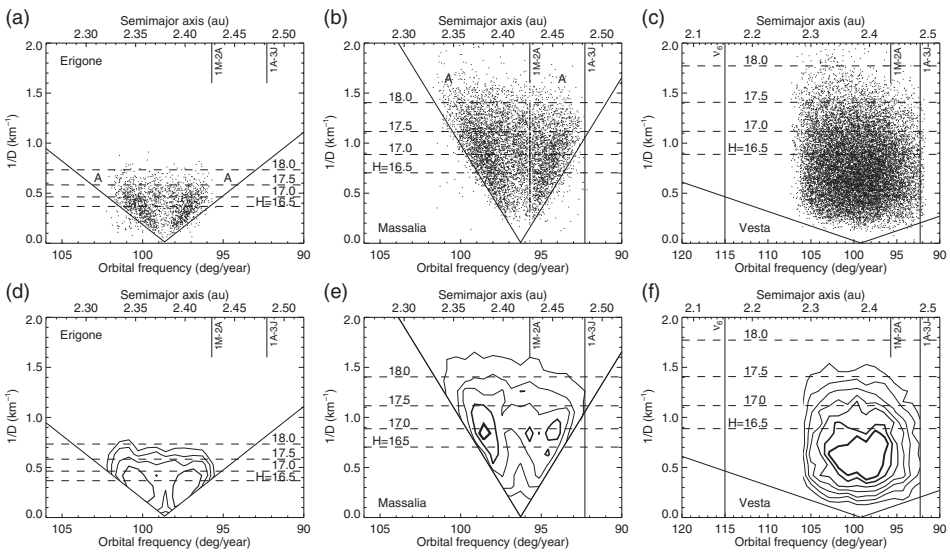

Figure 8. V-shaped distributions in $1/D - a$ space of the asteroids in the Erigone, Massalia and Vesta families with no limit on H. Diameters, D have been calculated assuming albedos of 0.06, 0.22 and 0.35 for, respectively, Erigone, Massalia and Vesta. The V-shaped lines for Massalia correspond to the fit determined by Milani *et al.* (2014). The lower panels are the corresponding number density plots with linear spacing of the contour plots.

surface crater counts (Marchi *et al.* 2012). However, the difference between these two age estimates could be even larger. Using the NEA orbital evolution timescale implies that the orbital evolution rates are constant, and we consider that to be unlikely. The NEA observations do not allow for asteroid disruptions or for changes in the asteroid spin directions and therefore the NEA observations are not applicable to the small asteroids in a family that is old. Thus, our estimate of the age of the Vesta family is likely to be a significant underestimate. We note that for both the high-inclination, non-family asteroids and the Vesta family, $t_{\rm evol}/T_{\rm Y} = 1/3$ (where $t_{\rm evol}$ is the average time of orbital evolution), consistent with our argument that both groups of asteroids have had similar evolutionary histories and therefore that both have ages comparable with the age of the solar system.

We support this conclusion by considering the dynamical evolution of small asteroids due to mechanisms other than Yarkovsky driven orbital evolution. The observations and models shown in Figs. 2, 4 and 7 reveal that the incremental SFDs of all the family and non-family asteroids are close to peaks at $H = 16.5$. For asteroids with $H < 16.5$, Yarkovsky loss is the dominant loss mechanism. The asteroids with $H > 16.5$ may not be observationally complete, but our models suggest that the number of small asteroids drops off sharply with increasing H. Small asteroids may be created by the disruption of larger asteroids, but this must be at a rate less than the loss rate. The distributions in $a - 1/D$ space of the asteroids in the Erigone, Massalia and Vesta families are shown in Fig. 8. The three sets of V-shaped lines correspond to ages of 1.6 10^8 Gyr (Erigone), 1.6 10^8 Gyr (Massalia) and 1.3 10^9 Gyr (Vesta). These ages were calculated using Yarkovsky timescales calculated from the NEA observations (Greenberg *et al.* 2020) for asteroids with $a = 2.4$ au, assuming asteroid densities of 1570 $kg\ m^{-3}$ (Erigone), 3000 $kg\ m^{-3}$ (Massalia) and 2850 $kg\ m^{-3}$ (Vesta, Jenniskens *et al.* (2021)). These three families were formed by cratering events (Spoto *et al.* 2015). However, their distributions in $a - 1/D$ space show significant differences. In Fig. 8a, we see that in the young Erigone family,

© in this web service Cambridge University Press & Assessment www.cambridge.org

CAMBRIDGE
Cambridge University Press & Assessment
978-1-108-49076-4 — Multi-scale (Time and Mass) Dynamics of Space Objects (IAU S364)
Edited by Alessandra Celletti, Cristian Beaugé, Cătălin Galeş, Anne Lemaître
Excerpt
More Information

the distribution of the larger asteroids with inverse diameters, $1/D \lesssim, 0.5$ has two well-separated lobes and a central depletion, consistent with orbital evolution at a constant rate driven by Yarkovsky forces without significant asteroid disruptions or changes in spin direction. However, for the smaller asteroids with $1/D \gtrsim 0.5$, we see an absence of a central depletion suggesting that these very small asteroids have experienced significant changes in their spin directions and/or collisional disruptions with the result that their orbital evolution may have been more of a random walk (Marzari *et al.* 2020; Dermott *et al.* 2021; Dell'Oro *et al.* 2021). We also see an absence of very small asteroids with high $1/D$ at the two extremes of the V-shaped distribution (marked in Fig. 8a with an A) suggesting, perhaps, that the very small asteroids in the family experienced disruptions preventing them from evolving to those extreme locations. However, this conclusion is not secure because any collisional disruption of the larger asteroids in the family would have produced an enhancement of the number density of small asteroids with high $1/D$ in the central region of the V-shaped distribution. In Fig. 8b, we observe that the young Massalia family has a distribution like that of the Erigone family, although for this family the loss of the central depletion occurs for those asteroids with $1/D \gtrsim 1.2$. Significantly, in Fig. 8c, we see that the distribution for the Vesta family is markedly different from both young families. For Vesta, the central depletion is absent at all diameters suggesting that most of the small asteroids in the Vesta family have experienced collisional evolution and/or significant changes in their spin directions, supporting our argument, based on the observed SFD, that the Vesta family could have an age comparable with the age of the solar system.

The plots in Fig. 8 for the Erigone and Massalia families contain information on the dynamical evolution of the families in addition to their ages. This may allow us to determine the timescale, T_{L} of the combined inclination-independent loss mechanisms separately from our estimate of the Yarkovsky loss timescale, but this information may only be useful when the observational completeness limit has been extended to, say, $H \sim 18$. The Erigone and Massalia families have approximately the same mean semimajor axis. Therefore, the degree of completeness of each family for a given value of H should be closely similar, although we note that the Erigone family has a mean eccentricity, $e = 0.191$ which is slightly greater than the mean value, $e = 0.142$, of the Massalia family, making the Erigone family asteroids slightly easier to discover. Current estimates of the observational completeness limit at $a = 2.4$ *au* are $H = 16.5$ (Dermott *et al.* 2018) and $H = 17.6$ (Hendler & Malhotra 2020). For families with ages greater than the timescale for the loss of asteroids of diameter D_{L} due to mechanisms other than Yarkovsky loss, we should observe a drop off in the number density of asteroids in $a - 1/D$ space of those asteroids with diameters $D < D_{\mathrm{L}}$, consistent with the observed shape of the SFD. For Erigone, which is a C-type asteroid with an albedo, A 0.06, there is a marked drop off in the number of asteroids with $H \gtrsim 17.0$, whereas for Massalia, which is an S-type asteroid with A 0.22, the drop off occurs for those asteroids with $H \gtrsim 18.0$. These values of H correspond to diameters $\sim$2.2 *km* for Erigone and $\sim$0.7 *km* for Massalia. While recognizing that for $H \gtrsim 17.0$ the distributions may be observationally incomplete, it is worth discussing the information that will be available when the completeness limit is extended to $H \sim 18.0$.

The Erigone and Massalia families both appear to have an age of $\sim$1.6 10^8 *Myr*, although this estimate assumes that the Yarkovsky timescale can be deduced from the NEA observations with allowance for the differences in the mean densities, but with no allowance for possible differences in their thermal efficiencies, even though these asteroids are of different types. We also note that the mean value of the thermal efficiencies of the NEAs is an average value that does not distinguish between NEAs of different types. The number of asteroids with $H < 16.5$ in the Massalia family is 1450, whereas the

© in this web service Cambridge University Press & Assessment www.cambridge.org